

# Test the two-pole structure of the $\Xi(1820)$ state

梁伟红

广西师范大学

2025 年轻强子专题研讨会

2025年5月8-12日, 安阳

---

**Based on:** R. Molina, WHL, C.W. Xiao, Z.F. Sun, E. Oset, PLB856 (2024) 138872;  
WHL, R. Molina, E. Oset, PRD110 (2024) 036005;  
M.Y. Duan, J. Song, WHL, E. Oset, EPJC84 (2024) 947.

# Outline

- ◆ Introduction: two-pole structure and the  $\Xi(1820)$  state
- ◆ Reactions testing the two states of  $\Xi(1820)$ 
  - $\psi(3686) \rightarrow \bar{\Xi}^+ K^- \Lambda$
  - $\psi(3686) \rightarrow \bar{\Xi}^+ \bar{K}^0 \Sigma^{*-} \rightarrow \bar{\Xi}^+ \bar{K}^0 \pi^- \Lambda$
  - $\Omega_c \rightarrow \pi \pi \Xi^*, \eta \pi \Xi^*$
- ◆ Summary

# ◆ Introduction: two-pole structure and the $\Xi(1820)$ state

## • Two-pole structure: $\Lambda(1405)$

Oller, Meißner, PLB500(2001)263;

Jido, Oller, Oset, Ramos, Meißner, NPA725(2003)181

Pseudoscalar meson – baryon( $\frac{1}{2}^+$ )  
interaction in  $S = -1$  sector, from  
LO of chiral Lagrangians.

Detailed review papers:

Meißner, Symmetry 12(2020)981;

Mai, Eur.Phys.J.ST 230 (2021)1593.

Other two-pole states:

$D_0^*(2300)$ ,  $K_1(1270)$ ,  $Y(4260)$ ,  $\dots$

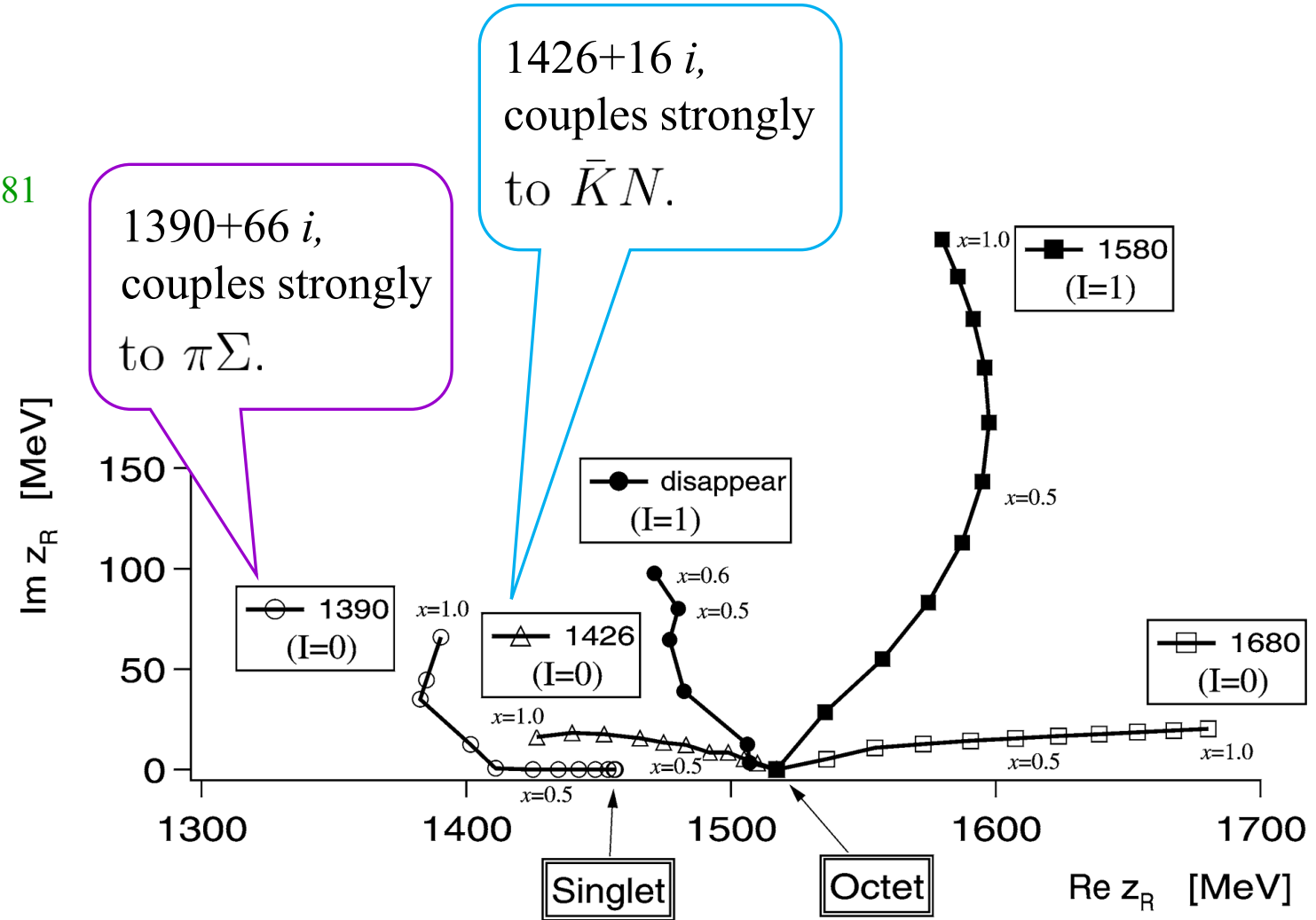


Fig. 1. Trajectories of the poles in the scattering amplitudes obtained by changing the SU(3) breaking parameter  $x$  gradually. At the SU(3) symmetric limit ( $x = 0$ ), only two poles appear, one is for the singlet and the other for the octets. The symbols correspond to the step size  $\delta x = 0.1$ .

# ◆ Introduction: two-pole structure and the $\Xi(1820)$ state

## • Two states of $\Xi(1820)$

The work of  $\Lambda(1405)$  was extended to pseudoscalar meson – baryon( $\frac{3}{2}^+$ ) interaction.

Four coupled channels :  $\Sigma^* \bar{K}$ ,  $\Xi^* \pi$ ,  $\Xi^* \eta$ ,  $\Omega K$   
 $(S = -2)$  [1878] [1669] [2078] [2165]

Transition potential:

$$V_{ij} = -\frac{1}{4f^2} C_{ij} (k^0 + k'^0); \quad f = 1.28 f_\pi, \quad f_\pi = 93 \text{ MeV},$$

Bethe-Salpeter (BS) equation:  $T = [1 - VG]^{-1} V$ .

$C_{ij}$	$\Sigma^* \bar{K}$	$\Xi^* \pi$	$\Xi^* \eta$	$\Omega K$
$\Sigma^* \bar{K}$	2	1	3	0
$\Xi^* \pi$		2	0	$\frac{3}{\sqrt{2}}$
$\Xi^* \eta$			0	$\frac{3}{\sqrt{2}}$
$\Omega K$				3

Sarkar, Oset, Vicente Vacas, NPA750(2005)294;  
Molina, WHL, Xiao, Sun, Oset, PLB856(2024) 138872.

**Table 2**

Pole positions and couplings for  $q_{\text{max}} = 830 \text{ MeV}$ .  
All quantities are given in units of MeV.

Poles	$ g_i $	$g_i$	channels
1824 – 31i	3.22	$3.22 - 0.096i$	$\bar{K} \Sigma^*$
	1.71	$1.55 + 0.73i$	$\pi \Xi^*$
	2.61	$2.58 - 0.38i$	$\eta \Xi^*$
	1.62	$1.47 + 0.67i$	$K \Omega$
1875 – 130i	2.13	$0.29 + 2.11i$	$\bar{K} \Sigma^*$
	3.04	$-2.07 + 2.23i$	$\pi \Xi^*$
	2.20	$1.11 + 1.90i$	$\eta \Xi^*$
	3.03	$-1.77 + 2.45i$	$K \Omega$

Two poles correspond to  $\Xi(1820)$ .

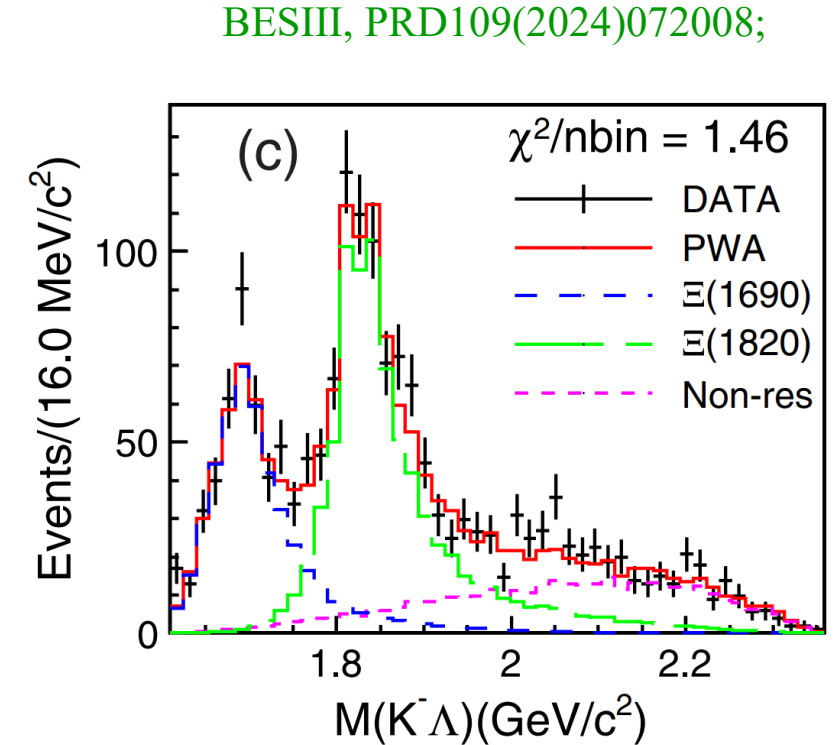
# ◆ Reactions testing the two states of $\Xi(1820)$ : $\psi(3686) \rightarrow \bar{\Xi}^+ K^- \Lambda$

- $\psi(3686) \rightarrow \bar{\Xi}^+ K^- \Lambda$

## ➤ New results from BESIII

TABLE VI. Results obtained for  $I(J^P)$ , mass and width for each component. The first (second) uncertainty is statistical (systematic).

Resonance	$I(J^P)$	M (MeV/ $c^2$ )	$\Gamma$ (MeV)
$\Xi(1690)^-$	$1/2(1/2^-)$	$1685_{-2}^{+3} \pm 12$	$81_{-9}^{+10} \pm 20$
$\Xi(1820)^-$	$1/2(3/2^-)$	$1821_{-3}^{+2} \pm 3$	$73_{-5}^{+6} \pm 9$



PDG estimate:  $M_{\Xi(1820)}^{\text{PDG}} = 1823 \pm 5 \text{ MeV}$ ,  $\Gamma_{\Xi(1820)}^{\text{PDG}} = \underline{24_{-10}^{+15}} \text{ MeV}$

The width of  $\Xi(1820)$  is much bigger, and incompatible with that of PDG!

One or two states for  $\Xi(1820)$ ?

# ◆ Reactions testing the two states of $\Xi(1820)$

➤ Two states of  $\Xi(1820)$  in  $\psi(3686) \rightarrow \bar{\Xi}^+ K^- \Lambda$

✓ The first test

The amplitude is of the type

$$t = \sum_{i,j} A_j \vec{e}_\psi \cdot \vec{p}_{\bar{\Xi}} G_j(P B^*) T_{ji} C_i \tilde{k}^2$$

$$\sim \sum_{i,j} D_{ij} \tilde{k}^2 \vec{e}_\psi \cdot \vec{p}_{\bar{\Xi}} T_{ji},$$

The invariant mass distribution:

$$\frac{d\Gamma}{dM_{\text{inv}}(K^- \Lambda)} = \frac{1}{(2\pi)^3} \frac{1}{4M_\psi^2} p_{\bar{\Xi}} \tilde{k} \sum |t|^2$$

$$= W p_{\bar{\Xi}}^3 \tilde{k}^5 \sum_{ij} |D_{ij} T_{ji}|^2,$$

Back ground:  $C p_{\bar{\Xi}} \tilde{k}$ ,

with  $W$  and  $C$  arbitrary weights.

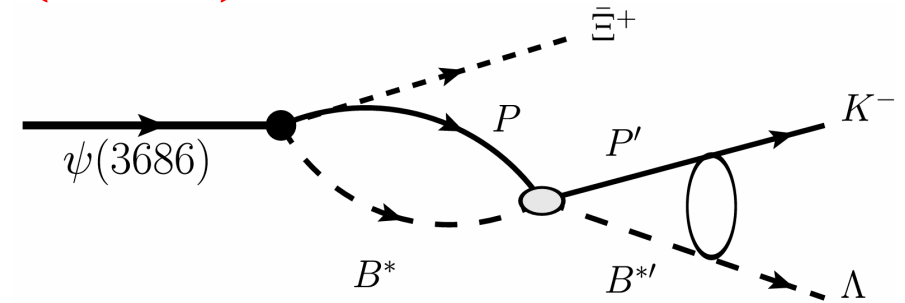


**Fig. 1.** The resonant mechanism for the production of  $\bar{\Xi}^+ K^- \Lambda$  in the  $\psi(3686)$  decay.  $P$  ( $P'$ ) and  $B^*$  ( $B^{*'} \text{)$  stand for pseudoscalar meson and decuplet baryon, respectively.

✓ The second test

$$\frac{A}{M_{\text{inv}} - M_{R_1} + i \frac{\Gamma_1}{2}} + \frac{B}{M_{\text{inv}} - M_{R_2} + i \frac{\Gamma_2}{2}},$$

R1, the narrower  $\Xi(1820)$  state with lower mass.

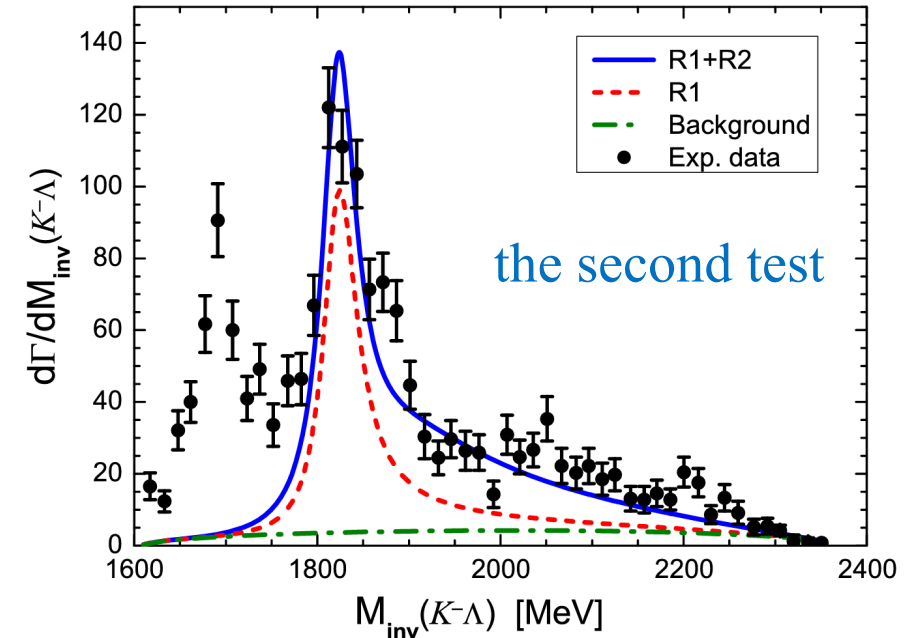
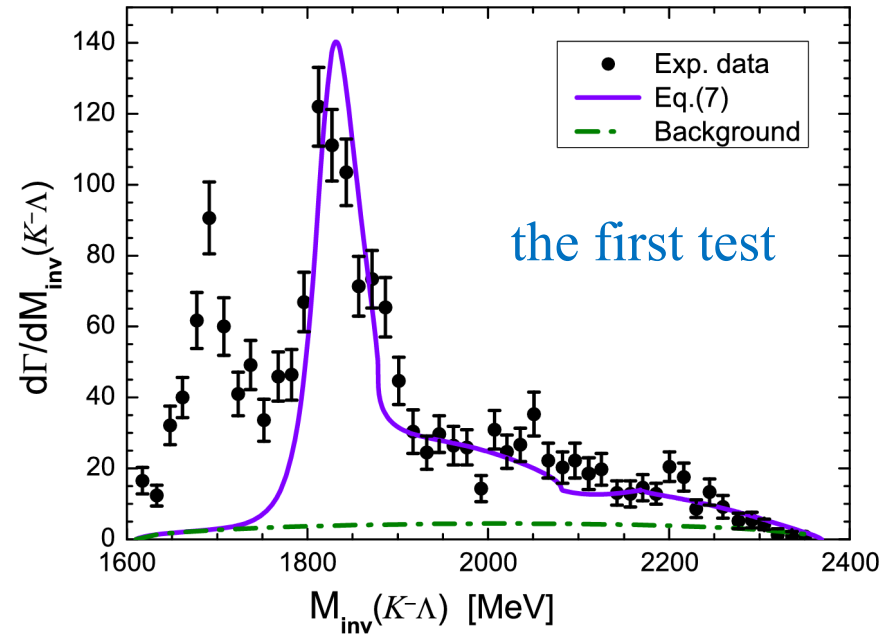
R2, the wider  $\Xi(1820)$  state with higher mass.

Adjust the coefficients  $A$  and  $B$  to fit the data.

# ◆ Reactions testing the two states of $\Xi(1820)$ : $\psi(3686) \rightarrow \bar{\Xi}^+ K^- \Lambda$

## ➤ Two states of $\Xi(1820)$ in $\psi(3686) \rightarrow \bar{\Xi}^+ K^- \Lambda$

- ✓ Same background in the two test cases.
- ✓ The coefficients  $A$  and  $B$  are found to have about the same strength.



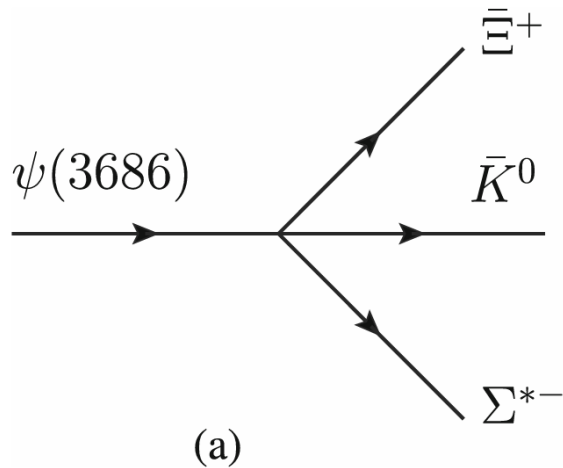
- ✓ A fair description of the data is obtained, supporting the two states of  $\Xi(1820)$ .
- ✓ Mostly the narrow resonance at 1824 MeV shows up, with the wider resonance providing strength in the higher energy region.

◆ Reactions testing the two states of  $\Xi(1820)$ :  $\psi(3686) \rightarrow \bar{\Xi}^+ \bar{K}^0 \Sigma^{*-} \rightarrow \bar{\Xi}^+ \bar{K}^0 \pi^- \Lambda$

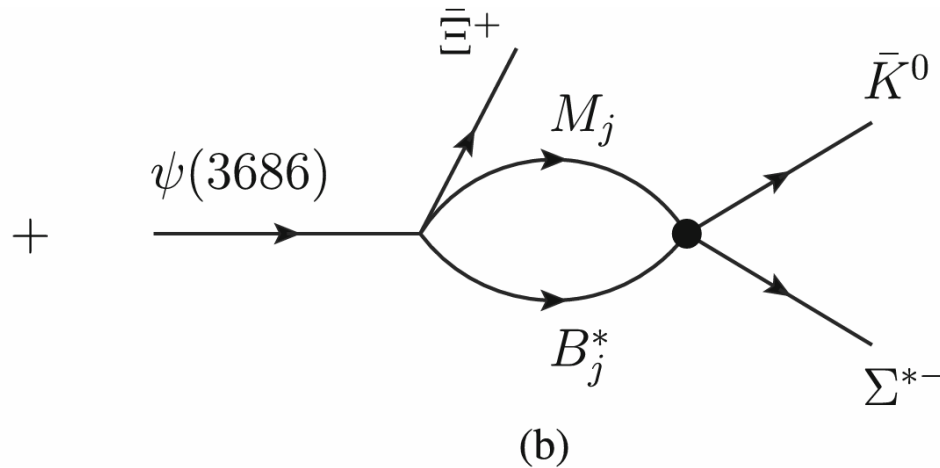
- $\psi(3686) \rightarrow \bar{\Xi}^+ \bar{K}^0 \Sigma^{*-} \rightarrow \bar{\Xi}^+ \bar{K}^0 \pi^- \Lambda$   
 $\downarrow$   
 with a threshold  $\sim 1880$  MeV

Coupled channels:  $\bar{K}^0 \Sigma^{*-}$ ,  $K^- \Sigma^{*0}$ ,  $\pi^0 \Xi^{*-}$ ,  $\eta \Xi^{*-}$ ,  $\pi^- \Xi^{*0}$ ,  $K^0 \Omega^-$

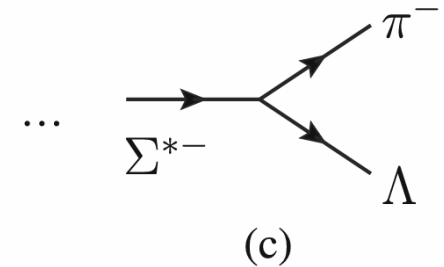
The mechanism for  $\psi(3686) \rightarrow \bar{\Xi}^+ \bar{K}^0 \Sigma^{*-}$ :



tree level



rescattering of the meson-baryon  
coupled channels



$\Sigma^{*-} \rightarrow \pi^- \Lambda$



# ◆ Reactions testing the two states of $\Xi(1820)$ : $\psi(3686) \rightarrow \bar{\Xi}^+ \bar{K}^0 \Sigma^{*-} \rightarrow \bar{\Xi}^+ \bar{K}^0 \pi^- \Lambda$

The decay amplitude for  $\psi(3686) \rightarrow \bar{\Xi}^+ \bar{K}^0 \Sigma^{*-}$ :

2-body scattering amplitudes

$$t = C \langle B^* | (\mathbf{S}^+ \times \mathbf{p}_{\bar{\Xi}^+}) \cdot \boldsymbol{\epsilon} | \Xi^- \rangle t', \quad t' = W_{\bar{K}^0 \Sigma^{*-}} + \sum_j W_j G_j t_{j, \bar{K}^0 \Sigma^{*-}},$$

$B^*$  is the baryon of the  $\frac{3}{2}^+$  multiplet,

$\boldsymbol{\epsilon}$  the vector polarization of the  $\psi(3686)$

$\mathbf{S}^+$  is the spin transition operator from spin  $\frac{1}{2}$  to  $\frac{3}{2}$

**Table 2**  $W_j$  Clebsch–Gordan coefficients for the different coupled channels

Channels	$\bar{K}^0 \Sigma^{*-}$	$K^- \Sigma^{*0}$	$\pi^0 \Xi^{*-}$	$\eta \Xi^{*-}$	$\pi^- \Xi^{*0}$	$K^0 \Omega^-$
$W_j$	$-\sqrt{\frac{2}{15}}$	$-\sqrt{\frac{1}{15}}$	$\sqrt{\frac{1}{15}}$	$-\sqrt{\frac{1}{5}}$	$-\sqrt{\frac{2}{15}}$	$\sqrt{\frac{2}{5}}$

The mass distribution for the decay  $\psi(3686) \rightarrow \bar{\Xi}^+ \bar{K}^0 \Sigma^{*-}$ :

$$\begin{aligned} \frac{d\Gamma}{dM_{\text{inv}}(\bar{K}^0 \Sigma^{*-})} &= \frac{1}{(2\pi)^3} \frac{1}{4M_\psi^2} p_{\bar{\Xi}^+} \tilde{p}_{\bar{K}^0} \sum \sum |t|^2 2M_{\bar{\Xi}^+} 2M_{\Sigma^{*-}} \\ &= \frac{1}{(2\pi)^3} \frac{C'}{4M_\psi^4} p_{\bar{\Xi}^+}^3 \tilde{p}_{\bar{K}^0} |t'|^2, \end{aligned}$$

◆ **Reactions testing the two states of  $\Xi(1820)$ :**  $\psi(3686) \rightarrow \bar{\Xi}^+ \bar{K}^0 \Sigma^{*-} \rightarrow \bar{\Xi}^+ \bar{K}^0 \pi^- \Lambda$

The mass distribution for  $\psi(3686) \rightarrow \bar{\Xi}^+ \bar{K}^0 \Sigma^{*-} \rightarrow \bar{\Xi}^+ \bar{K}^0 \pi^- \Lambda$  :

$$\begin{aligned} & \frac{d\Gamma}{dM_{\text{inv}}(\bar{K}^0 \Sigma^{*-}) dM_{\text{inv}}(\Sigma^{*-})} \\ &= -\frac{1}{\pi} \text{Im} \frac{\frac{\Gamma_{\pi^- \Lambda}}{\Gamma_{\Sigma^{*-}}}}{M_{\text{inv}}(\Sigma^{*-}) - M_{\Sigma^{*-}} + i \frac{\Gamma_{\Sigma^{*-}}(M_{\text{inv}}(\Sigma^{*-}))}{2}} \cdot \frac{1}{(2\pi)^3} \frac{C'}{4M_\psi^4} p_{\bar{\Xi}^+}^3 \tilde{p}_{\bar{K}^0} |t'|^2, \end{aligned}$$

with the energy dependence of the  $\Sigma^{*-}$  width as

$$\Gamma_{\Sigma^{*-}}(M_{\text{inv}}(\Sigma^{*-})) = \Gamma_{\text{on}} \frac{M_{\Sigma^{*-}}}{M_{\text{inv}}(\Sigma^{*-})} \left( \frac{\tilde{p}_\pi}{\tilde{p}_{\pi, \text{on}}} \right)^3,$$

with  $\Gamma_{\text{on}}$  the width of  $\Sigma^{*-}$ ,  $\Gamma_{\pi^- \Lambda} / \Gamma_{\Sigma^{*-}} = 87\%$ .

$$\tilde{p}_\pi = \frac{\lambda^{1/2}(M_{\text{inv}}^2(\Sigma^{*-}), m_\pi^2, m_\Lambda^2)}{2 M_{\text{inv}}(\Sigma^{*-})}, \quad \tilde{p}_{\pi, \text{on}} = \frac{\lambda^{1/2}(m_{\Sigma^{*-}}^2, m_\pi^2, m_\Lambda^2)}{2 m_{\Sigma^{*-}}}.$$

# ◆ Reactions testing the two states of $\Xi(1820)$ : $\psi(3686) \rightarrow \bar{\Xi}^+ \bar{K}^0 \Sigma^{*-} \rightarrow \bar{\Xi}^+ \bar{K}^0 \pi^- \Lambda$

- ✓ There is destructive interference of the tree level and the two  $\Xi(1820)$  states.
- ✓ The actual mass distribution differs appreciably from phase space.
- ✓ The phase space for  $\bar{K}^0 \Sigma^{*-}$  production reduces the effect of the lower mass  $\Xi(1820)$ .
- ✓ The excess of strength above 1900 MeV is due to the wide  $\Xi(1820)$  state with higher mass.

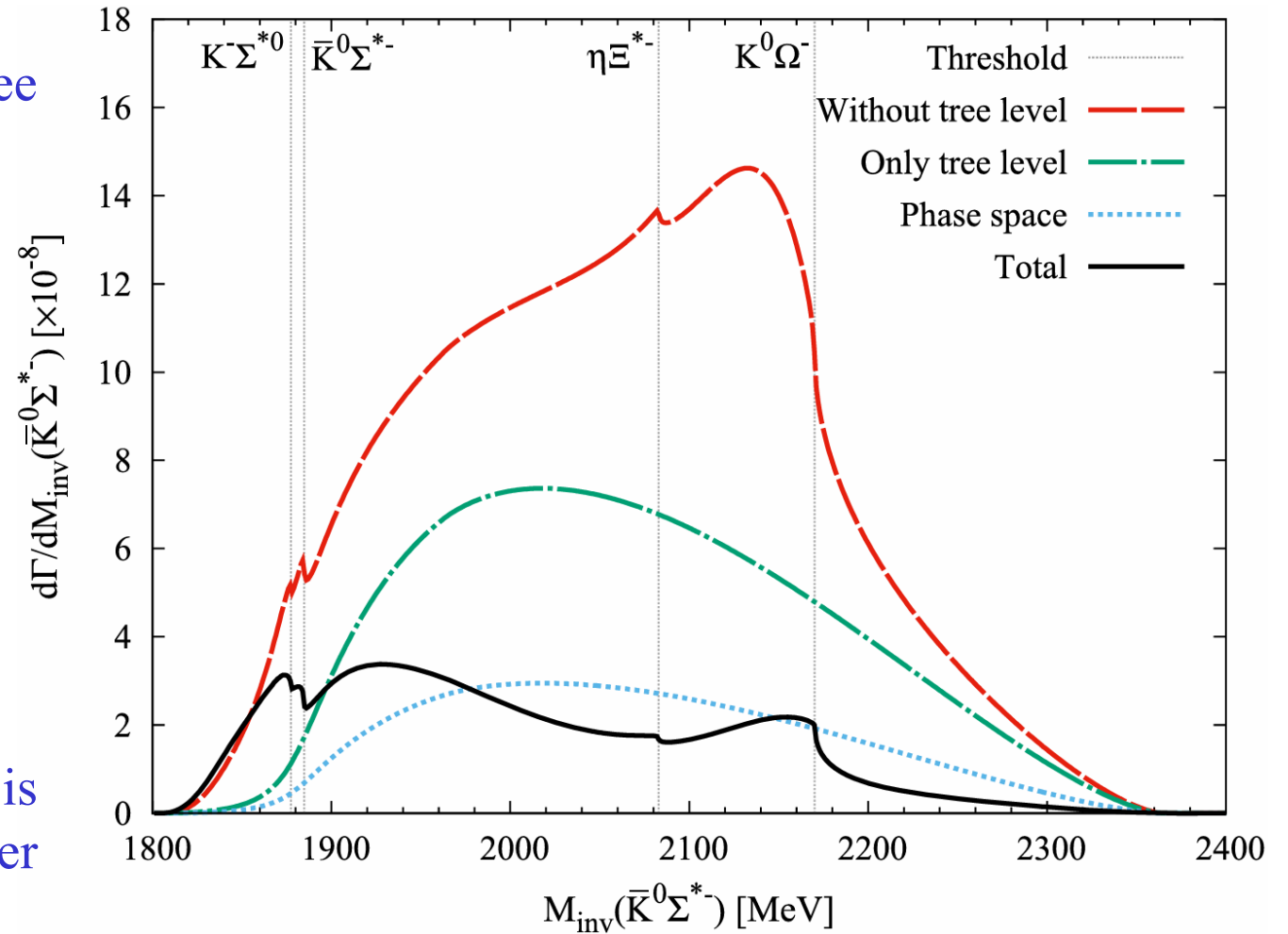


**Fig. 2**  $d\Gamma/dM_{\text{inv}}(\bar{K}^0 \Sigma^{*-})$  with different options.

The proposed reaction is particularly suited to show the effect of the higher  $\Xi(1820)$  state.

◆ Reactions testing the two states of  $\Xi(1820)$ :  $\Omega_c^0 \rightarrow \pi(\eta)\pi\Xi^*$

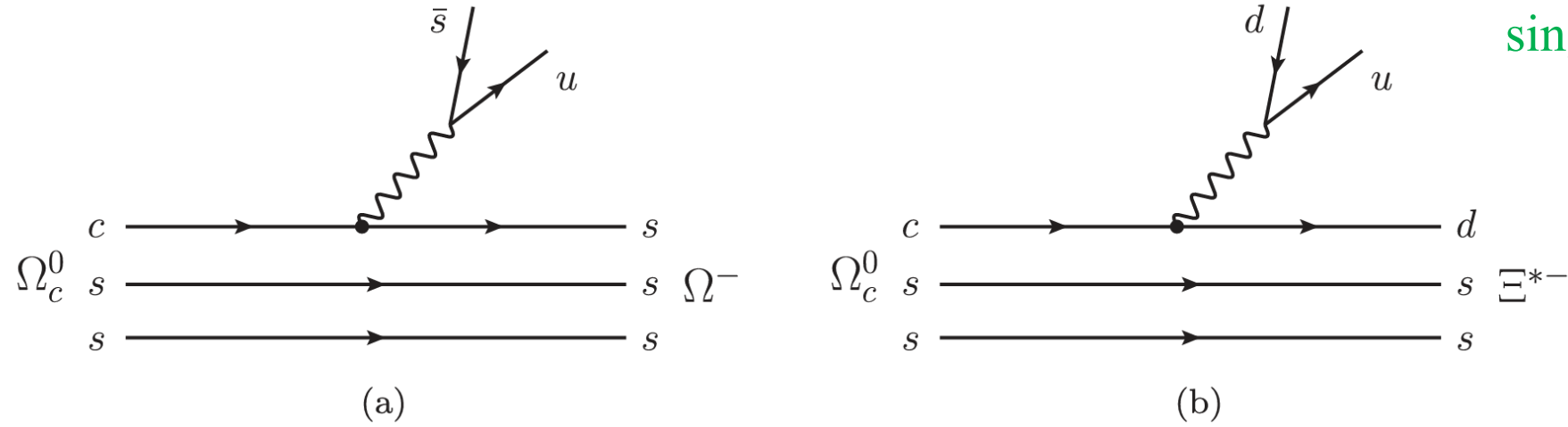


FIG. 1. The two topological structures with external emission that lead to  $\Omega^-$  (a) and  $\Xi^{*-}$  (b) in the final state.

Hadronization:

$$u\bar{s} \rightarrow \sum_i u\bar{q}_i q_i \bar{s} = P_{1i} P_{i3} = (P^2)_{13} = \left( \frac{\pi^0}{\sqrt{2}} + \frac{\eta}{\sqrt{3}} \right) K^+ + \pi^+ K^0 - \frac{1}{\sqrt{3}} K^+ \eta.$$

$$u\bar{d} \rightarrow \sum_i u\bar{q}_i q_i \bar{d} = P_{1i} P_{i2} = (P^2)_{12} = \left( \frac{\pi^0}{\sqrt{2}} + \frac{\eta}{\sqrt{3}} \right) \pi^+ + \pi^+ \left( -\frac{\pi^0}{\sqrt{2}} + \frac{\eta}{\sqrt{3}} \right) + K^+ \bar{K}^0.$$

$$P = \begin{pmatrix} \frac{\pi^0}{\sqrt{2}} + \frac{\eta}{\sqrt{3}} & \pi^+ & K^+ \\ \pi^- & -\frac{\pi^0}{\sqrt{2}} + \frac{\eta}{\sqrt{3}} & K^0 \\ K^- & \bar{K}^0 & -\frac{\eta}{\sqrt{3}} \end{pmatrix},$$

◆ Reactions testing the two states of  $\Xi(1820)$ :  $\Omega_c^0 \rightarrow \pi(\eta)\pi\Xi^*$

with a threshold  $\sim 1670$  MeV

To generate the  $\Xi(1820)$  resonance in the final state, we have to allow one of the mesons to interact with the  $\Omega^-$  or  $\Xi^{*-}$ .

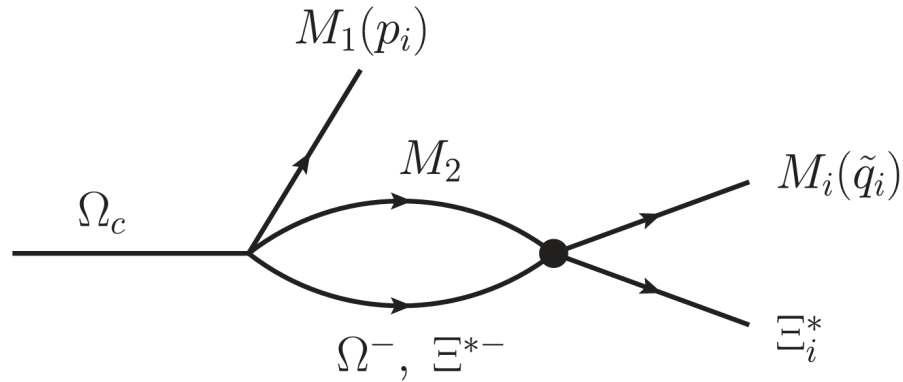


FIG. 2. Final state interaction of a meson with the baryon of the decuplet  $3/2^+$ . The dot indicates the transition matrix element from  $M_2\Omega^-(\Xi^{*-})$  to a final  $M_i\Xi_i^*$  state.

We have 6 possible reactions:

$$\Omega_c^0 \rightarrow \pi^+ \pi^0 \Xi^{*-} \text{ (with tree level)}$$

$$\Omega_c^0 \rightarrow \pi^+ \pi^- \Xi^{*0}$$

$$\Omega_c^0 \rightarrow \pi^0 \pi^+ \Xi^{*-} \text{ (with tree level)}$$

$$\Omega_c^0 \rightarrow \pi^0 \pi^0 \Xi^{*0}$$

$$\Omega_c^0 \rightarrow \eta \pi^+ \Xi^{*-}$$

$$\Omega_c^0 \rightarrow \eta \pi^0 \Xi^{*0}$$

where the first meson corresponds to the external one of the weak vertex and the second one to the final state.

◆ Reactions testing the two states of  $\Xi(1820)$ :  $\Omega_c^0 \rightarrow \pi(\eta)\pi\Xi^*$

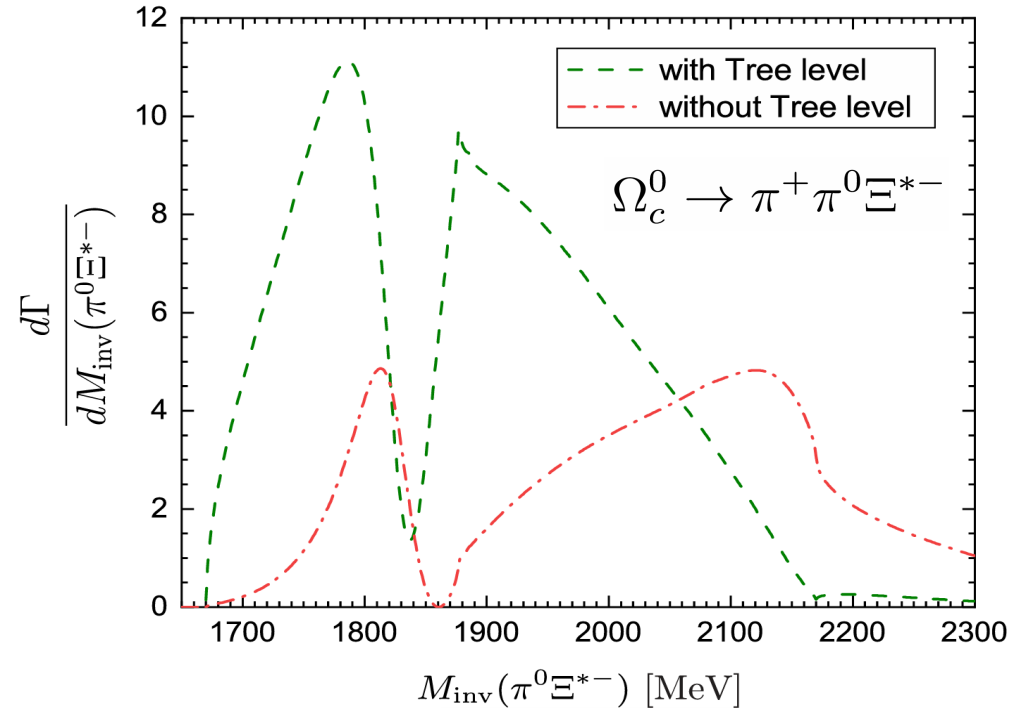
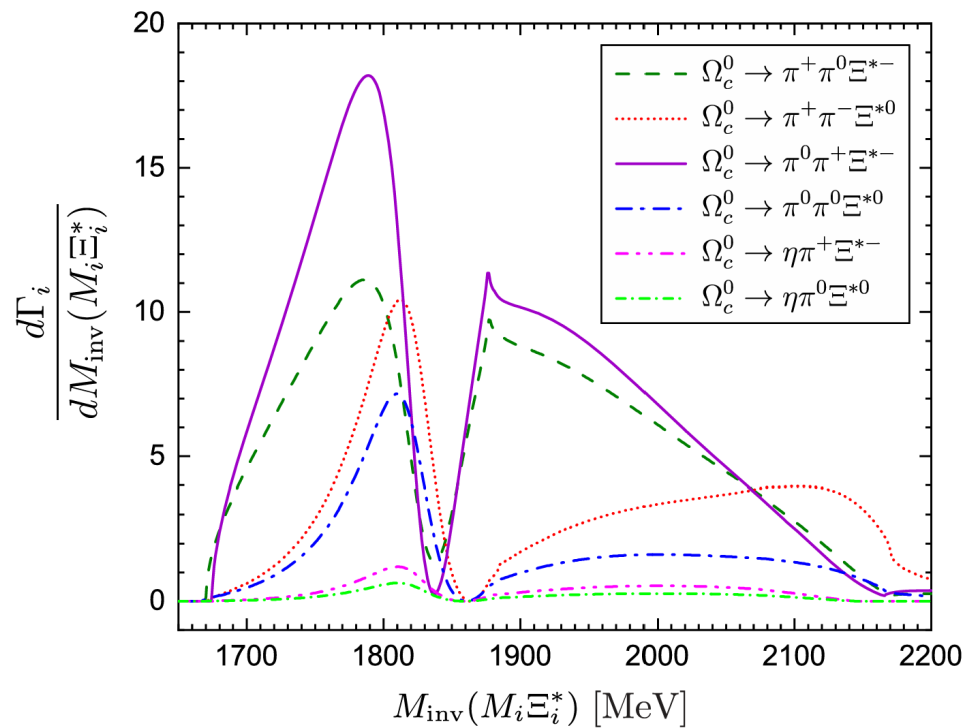
---

The mass distribution for the final  $M_i\Xi_i^*$  pair is given by

$$\frac{d\Gamma_i}{dM_{\text{inv}}(M_i\Xi_i^*)} = \frac{1}{(2\pi)^3} \frac{1}{4M_{\Omega_c}^2} p_i \tilde{q}_i \bar{\sum} \sum |t_i|^2 \quad (i = 1 \sim 6),$$

$$t_i = C \langle \Xi^*(3/2^+) | \vec{S}^+ \cdot \vec{p}_i | \Omega_c^0 \rangle \tilde{t}_i, \quad \bar{\sum} \sum |t_i|^2 = C^2 \frac{2}{3} \vec{p}_i^2 |\tilde{t}_i|^2.$$

# ◆ Reactions testing the two states of $\Xi(1820)$ : $\Omega_c^0 \rightarrow \pi(\eta)\pi\Xi^*$



- ✓ The shapes of the mass distributions for the reactions are different from each other.
- ✓ In common: there is a dip in the mass distribution around 1850 MeV, due to the destructive interference of the two resonances.
- ✓ The reactions without tree level contribution, show more clearly the effect of the two  $\Xi(1820)$  state.

## ◆ Summary

- ✓ The chiral unitary approach for the interaction of pseudoscalar mesons with the baryons of the decuplet predicts two states for the  $\Xi(1820)$ , one at 1824 MeV with a width of 62 MeV, and a second one at 1875 MeV with a large width of 260 MeV.
- ✓ With the contribution of the two  $\Xi(1820)$  states, a fair description of the BESIII data for the  $\psi(3686) \rightarrow \bar{\Xi}^+ K^- \Lambda$  decay is obtained, supporting the two-pole structure of the  $\Xi(1820)$  state.
- ✓ We propose the reaction  $\psi(3686) \rightarrow \bar{\Xi}^+ \bar{K}^0 \Sigma^{*-} \rightarrow \bar{\Xi}^+ \bar{K}^0 \pi^- \Lambda$  to show evidence for the existence of two  $\Xi(1820)$  states. The phase space for  $\bar{K}^0 \Sigma^{*-}$  production reduces the effect of the lower mass state, magnifying the effect of the higher mass state that shows clearly over the phase space.
- ✓ The  $\Omega_c^0 \rightarrow \pi^+ \pi^- \Xi^{0*}, \pi^0 \pi^0 \Xi^{0*}, \eta \pi^+ \Xi^{*-}, \eta \pi^0 \Xi^{*0}$  decays, being free of a tree level contribution, show clearly the effect of the two  $\Xi(1820)$  state. The lower mass one is clearly seen as a sharp peak in the  $\pi \Xi^*$  mass distributions, but the higher mass one manifests itself through an interference with the lower one that leads to a dip in the mass distribution around 1850 MeV.

**Thank you for your attention!**